



Contents lists available at ScienceDirect

## Protein Expression and Purification

journal homepage: [www.elsevier.com/locate/yprep](http://www.elsevier.com/locate/yprep)Expression of soluble and functional human neonatal Fc receptor in *Pichia pastoris*Chang-Han Lee<sup>a</sup>, Dong-Ki Choi<sup>b</sup>, Hye-Ji Choi<sup>b</sup>, Moo-Young Song<sup>c</sup>, Yong-Sung Kim<sup>a,b,\*</sup><sup>a</sup> Dept. of Molecular Science and Technology, Ajou University, San 5, Woncheon-dong, Yeongtong-gu, Suwon 443-749, Republic of Korea<sup>b</sup> Dept. of Applied Chemistry and Biological Engineering, Ajou University, San 5, Woncheon-dong, Yeongtong-gu, Suwon 443-749, Republic of Korea<sup>c</sup> Biotech Laboratory, Yuhan Research Institute, Yuhan Inc., 416-1 Giheung, Yongin, Republic of Korea

## ARTICLE INFO

## Article history:

Received 26 September 2009

and in revised form 30 November 2009

Available online 16 December 2009

## Keywords:

Neonatal Fc receptor

Two-promoter vector system

*Pichia pastoris*

Functional expression

Fc engineering

## ABSTRACT

The neonatal Fc receptor (FcRn) is a non-covalently associated heterodimeric protein composed of a transmembrane anchored heavy chain ( $\alpha$ FcRn) and a soluble light chain  $\beta$ 2-microglobulin ( $\beta$ 2m). In addition to its role in the transfer of maternal immunoglobulin Gs (IgGs) to the fetus, FcRn plays a key role in prolonging the serum half-life of IgGs *in vivo*. Herein, we report a strategy for functional expression of soluble human FcRn (shFcRn) in *Pichia pastoris* using a two-promoter vector system, where  $\alpha$ FcRn and  $\beta$ 2m are co-expressed under their respective promoters in a single vector. The purified shFcRn from the culture supernatants correctly assembled to form the heterodimer with the typical secondary structures. At acidic pHs between 5.0 and 6.4, shFcRn exhibited substantial binding to the four subclasses of human IgGs at acidic pHs between 5.0 and 6.4, but at pHs between 6.8 and 8.0, its binding was negligible. No cross-reactivity with mouse IgG was exhibited even at acidic pH. This was consistent with the pH-dependent binding profiles of the shFcRn prepared from the mammalian cell expression. Furthermore, the shFcRn exhibited about 10-fold higher binding affinity with the tumor necrosis factor- $\alpha$  antagonists of monoclonal antibodies Infliximab and Adalimumab than that of Etanercept, providing a clue to their different serum half-lives *in vivo*. Our results suggest that the functionally expressed shFcRn from *Pichia* can be used for the biochemical and biological studies and as a screening probe for Fc engineering of human IgGs.

© 2009 Elsevier Inc. All rights reserved.

## 1. Introduction

The neonatal Fc receptor (FcRn)<sup>1</sup> is a non-covalently associated heterodimeric protein composed of a transmembrane anchored  $\alpha$ -heavy chain ( $\alpha$ FcRn) and a soluble light chain  $\beta$ 2-microglobulin ( $\beta$ 2m). It is expressed ubiquitously in endothelial cells of human tissues (reviewed in Refs. [1,2]). FcRn transfers immunoglobulin Gs (IgGs) from mother to offspring across the placenta during gestation and also plays a central role in the regulation of IgG serum levels in adults [1–3]. These two critical functions of FcRn are explained by its strict pH-dependent binding interactions with IgGs. The Fc portion of IgG binds with high affinity to FcRn at an acidic pH (5.0–6.5) but not at a physiological pH (7.0–7.4) [4,5]. Internalized IgGs by fluid-phase pinocytosis in endothelial cells are bound by FcRn in acidified endosomes, recycled back to the cell surface, and released from FcRn

into the circulation at the physiological pH [1,2]. Thus FcRn intercepts IgGs that are otherwise destined for lysosomal degradation, extending their serum half-lives in the circulation much longer than non-IgG proteins.

Efforts have recently been undertaken to modulate human IgG (hIgG) serum half-life by engineering the Fc portion to have altered affinities for human FcRn (hFcRn) [6–8]. In addition to the Fc engineering purpose, detailed biochemical and biological studies of hFcRn require large amounts of soluble human FcRn (shFcRn). Recombinant shFcRn has been solubly expressed by co-transfection of two vectors encoding  $\beta$ 2m and the extracellular region of  $\alpha$ FcRn, respectively, into human embryonic cells [7], Chinese hamster ovarian (CHO) cells [4,9], and insect cells [10,11]. Due to the high cost and time-consuming processes of the mammalian expression system, bacterial expression of shFcRn has been recently reported as an alternative [12]. However, both  $\beta$ 2m and  $\alpha$ FcRn are insolubly expressed as inclusion bodies in *Escherichia coli*, requiring laborious refolding procedures to prepare the assembled shFcRn [12,13].

Herein, we describe soluble and functional expression of shFcRn in *Pichia pastoris* using a two-promoter vector that co-expresses  $\beta$ 2m and  $\alpha$ FcRn under their respective promoters in a single vector. We found that  $\beta$ 2m and  $\alpha$ FcRn were solubly expressed to form correctly assembled heterodimeric shFcRn, which showed the typical

\* Corresponding author. Address: Dept. of Molecular Science and Technology, Ajou University, San 5, Woncheon-dong, Yeongtong-gu, Suwon 443-749, Republic of Korea. Fax: +82 31 219 1610.

E-mail address: [kimys@ajou.ac.kr](mailto:kimys@ajou.ac.kr) (Y.-S. Kim).

<sup>1</sup> Abbreviations used: Fc, fragment crystallizable; FcRn, neonatal Fc receptor;  $\alpha$ FcRn, FcRn heavy chain;  $\beta$ 2m,  $\beta$ 2-microglobulin; shFcRn, soluble human FcRn; TNF $\alpha$ , tumor necrosis factor- $\alpha$ ; mAb, monoclonal antibody; IgG, immunoglobulin G; hIgG, human IgG; mIgG, mouse IgG; SPR, surface plasmon resonance.

pH-dependent binding patterns for the four subclasses of hlgG. Furthermore, the binding analyses of shFcRn with tumor necrosis factor- $\alpha$  (TNF $\alpha$ ) antagonists [14,15], including Infliximab (Remicade<sup>®</sup>), Adalimumab (Humira<sup>®</sup>), and Etanercept (Enbrel<sup>®</sup>), provide a clue toward explaining the differences between their serum half-lives.

## 2. Materials and methods

### 2.1. Materials

Restriction enzymes and high fidelity DNA polymerase were purchased from New England Biolabs (MA, USA). As a DNA molecular weight marker, a 1-kb ladder from Invitrogen was used. Infliximab (Remicade<sup>®</sup>, Johnson & Johnson), Adalimumab (Humira<sup>®</sup>, Abbott), and Etanercept (Enbrel<sup>®</sup>, Amgen) were provided by a commercial supplier [14]. The oligodeoxynucleotides were synthesized at Bioneer Co. (Taejon, Korea). All of the other chemicals and solvents used were of analytical grade, unless otherwise specified.

### 2.2. Construction of a two-promoter vector for the co-expression $\alpha$ FcRn and $\beta$ 2m in *Pichia*

A soluble extracellular portion of human  $\alpha$ FcRn (residues 1–267 of the mature protein) (hereafter designated  $\alpha$ FcRn) and human  $\beta$ 2m (126 residues) were amplified with primer sets of HCF and HCR for  $\alpha$ FcRn and  $\beta$ 2mF and  $\beta$ 2mR for  $\beta$ 2m (Table 1) and subcloned into a *Pichia* expression pPICZ $\alpha$ A vector (Invitrogen) with *NheI*/*XbaI* sites for  $\alpha$ FcRn and *NheI*/*BamHI* sites for  $\beta$ 2m, resulting in pPICZ $\alpha$ A- $\alpha$ FcRn and pPICZ $\alpha$ A- $\beta$ 2m, respectively. The *PmeI* site (5'-GTT TAA AC-3') of AOX1 promoter in pPICZ $\alpha$ A- $\beta$ 2m was point-mutated as 5'-GTT GAA AC-3', where the mutated site was underscored by underline, using a site-directed mutagenesis kit (Stratagene) with a primer set (PmeF = 5'-CAA ATG GCC CAA AAC TGA CAG TTG AAA CGT CTT GGA ACC TAA TAT GAC-3') and PmeR = 5'-GTC ATA TTA GGT TCC AAG ACG TTT CAA CTG TCA GTT TTG GGC CAT TTG-3'). Then the fragment containing the alcohol oxidase (AOX1) promoter, MF $\alpha$  secretion signal peptide, and  $\beta$ 2m in pPICZ $\alpha$ A- $\beta$ 2m was amplified with a primer set of  $\beta$ 2m2cisF and  $\beta$ 2m2cisR and subcloned into the pPICZ $\alpha$ A- $\alpha$ FcRn with *XbaI* site, resulting in a pPICZ $\alpha$ A- $\alpha$ FcRn- $\beta$ 2m (Fig. 1A). The 5'-terminus of  $\beta$ 2m2cisF primer encodes the Flag tag sequence, stop codon and space sequence prior to the AOX1 promoter (Table 1). The construct was confirmed by sequencing.

### 2.3. Transformation and PCR analysis of a *Pichia* transformant

The plasmid of pPICZ $\alpha$ A- $\alpha$ FcRn- $\beta$ 2m was linearized with *PmeI* and then transformed into *P. pastoris* GS115 strain by electroporation

**Table 1**  
Primer sequences used in this study.<sup>a</sup>

Primers	Sequence
HCF	5'-CGC TAG CGC AGA AAG CCA CCT CTC CCT CC-3'
HCR	5'-AAT CTA GAC AGC TCC ACC CTG AGG GGC-3'
$\beta$ 2mF	5'-CGC TAG CAT CCA GCG TAC TCC AAA GAT TCA GG-3'
$\beta$ 2mR	5'-TGG ATC CCA TGT CTC GAT CCC ACT TAA CTA TCT TG-3'
$\beta$ 2m2cisF <sup>b</sup>	5'-AAT TCT AGA CTT AAG GAC TAC AAG GAC GAT GAC AAG TAA GAC TGG TTC CAA TTG ACA AGC TTT TGA T-3'
$\beta$ 2m2cisR	5'-ATL CTA GAC ATG TCT CGA TCC CAC TTA ACT ATC T-3'

<sup>a</sup> Enzyme restriction sites were highlighted by underlines.

<sup>b</sup> The Flag tag was highlighted by bolded characters.

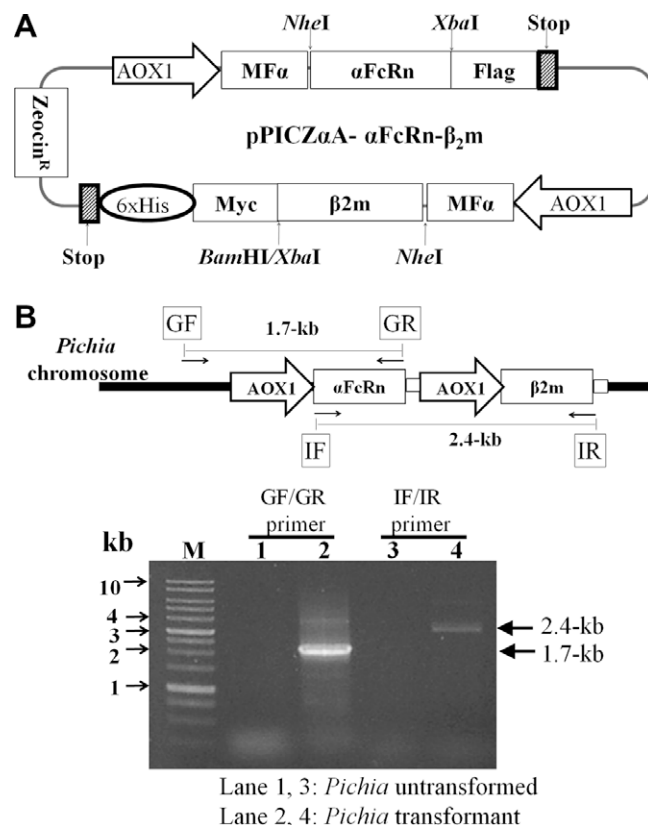


**Fig. 1.** (A) Schematic diagram showing the two-promoter expression vector for the expression  $\alpha$ FcRn and  $\beta$ 2m under the respective promoter in a single vector in *Pichia*. AOX1, AOX1 promoter; MF $\alpha$ , mating factor- $\alpha$  secretion signal peptide;  $\alpha$ FcRn, the soluble region of hFcRn heavy chain;  $\beta$ 2m,  $\beta$ 2-microglobulin; Flag, Flag tag; Myc, c-Myc tag; 6xHis, six His tag; Stop, translational stop sequence. (B) Analysis of the plasmid integration into the AOX1 gene of *Pichia* genome by genomic PCRs using the indicated primer sets. The size of amplified PCR product was indicated by arrows. Lane M, molecular weight marker of 1-kb ladder; Lanes 1 and 3, control *Pichia* untransformed; Lanes 2 and 4, the chosen *Pichia* transformant. The expected size of PCR product by a GF and GR primer set (1.7-kb) or by an IF and IR primer set (2.4-kb) was indicated in the upper panel. The details were described in the text.

according to the EasySelect<sup>™</sup> *Pichia* expression kit (Invitrogen). For the selected zeocin-resistant colonies, initial screening of the culture supernatants by SDS-PAGE analysis was carried out to identify a yeast clone showing the highest expression level of shFcRn. The chosen *Pichia* transformant was analyzed by genomic PCRs to confirm the site of integration of plasmid pPICZ $\alpha$ A- $\alpha$ FcRn- $\beta$ 2m. Genomic DNA was prepared using a Easy-DNA<sup>™</sup> kit (Invitrogen) following the manufacture protocol and used as template in PCR using two primer sets: One is GF (5'-GCT CGT ACG AGA AGA AAC AAA ATG A-3') and GR (5'-CAG CTC CAC CCT GAG GGG-3') and the other is IF (5'-GCA GAA AGC CAC CTC TCC CT-3') and IR (5'-CAT GTC TCG ATC CCA CTT AAC TAT C-3'). The GF and GR primers correspond to sequences present upstream (-121 bp) of AOX1 promoter and 3'-terminus region of  $\alpha$ FcRn, respectively (Fig. 1B). The IF primer was designed based on the genome sequence recently archived [16]. The IF and IR primers anneal to the 5'-terminus region of  $\alpha$ FcRn and 3'-terminus region of  $\beta$ 2m, respectively (Fig. 1B). PCRs using *Taq* polymerase (1.25 U) were performed in 50- $\mu$ l solutions containing yeast genomic DNA (1  $\mu$ g), primers (0.5  $\mu$ g), deoxynucleotide triphosphates (500  $\mu$ M), and MgCl<sub>2</sub> (2 mM).

### 2.4. Expression and purification of shFcRn

For shFcRn expression, the chosen yeast clone was grown at 30 °C to an OD<sub>600</sub> of ~20 in BMGY medium (1% yeast extract, 2%

peptone, 100 mM potassium phosphate (pH 6.0), 1.34% yeast nitrogen base,  $4 \times 10^{-5}$ % biotin, 1% glycerol) plus zeocin (100  $\mu\text{g}/\text{ml}$ ) and then induced for 72 h at 30 °C in BMMY medium (1% yeast extract, 2% peptone, 100 mM potassium phosphate (pH 6.0), 1.34% yeast nitrogen base,  $4 \times 10^{-5}$ % biotin, 0.5% methanol) plus zeocin (100  $\mu\text{g}/\text{ml}$ ) in a 2-liter flask containing 400 ml of medium. Then,  $\alpha\text{FcRn}$  and  $\beta 2\text{m}$  were co-purified from the culture supernatant using anti-6 $\times$ His tag at the C-terminus of  $\beta 2\text{m}$  (Talon resin, Clontech) [14,17]. The purified proteins were extensively dialyzed against PBS (137 mM NaCl, 2.7 mM KCl, 10 mM  $\text{Na}_2\text{HPO}_4$ , 2 mM  $\text{KH}_2\text{PO}_4$ , pH 7.4) at 4 °C. The protein concentrations were determined using the Bradford protein assay.

The purified proteins were analyzed by 12% SDS-PAGE under the non-reducing condition and typically found to have greater than 90% purity. Treatment of the purified shFcRn with endoglycosidase PNGase F (New England Biolabs) was performed at 37 °C for 1 h according to the manufacturer's instructions in 50- $\mu\text{l}$  enzyme buffer containing denatured shFcRn proteins (30  $\mu\text{g}$ ) and PNGase F (500 unit). As a positive control, Infliximab mAb was treated under the same condition. The samples were analyzed on 12% reducing SDS-PAGE.

### 2.5. Size exclusion chromatography (SEC)

SEC analysis of the purified shFcRn was performed on an Agilent 1100 high performance liquid chromatography system using a SuperdexTM200 10/300GC (GE Healthcare), with a mobile phase of PBS (pH 7.4) at a flow rate of 0.5 ml/min [14,17], as described in detail in the Figure legend. A set of molecular mass standard markers (Sigma) ranging from 13.7 to 66 kDa was used.

### 2.6. Far-UV circular dichroism (CD) spectroscopy

Far-UV CD spectrum (190–260 nm) of the purified shFcRn (100  $\mu\text{g}/\text{ml}$  in PBS, pH 7.4) was recorded on a J-715 spectropolarimeter (Jasco Inc., Japan) at 25 °C in a 0.1-cm path length quartz cuvette with a step size of 0.5 nm and processed as previously described [17].

### 2.7. Binding of shFcRn with hlgGs and TNF $\alpha$ antagonists by ELISA

Binding specificity and affinity of shFcRn to the four subclasses of hlgG (IgG1, IgG2, IgG3 and IgG4) (Calbiochem) and TNF $\alpha$  antagonists (Infliximab, Adalimumab, and Etanercept) were determined by ELISA [18], using mouse IgG (mIgG) (Sigma) as a negative control. The concentrations of hlgGs, mIgG and TNF $\alpha$  antagonists were determined using the known extinction coefficient by measuring  $\text{OD}_{280}$  [7,14]. In concentration-dependent binding ELISAs, ELISA plates (Nunc, Invitrogen) were coated with 1  $\mu\text{g}/\text{ml}$  of each protein (hlgGs, mIgG and TNF $\alpha$  antagonists) overnight at 4 °C and blocked with 1% (w/v) skim milk (Sigma). After washing with PBST (PBS, pH 6.0, plus 0.01% Tween-20), serially diluted shFcRn (0.5 nM–50  $\mu\text{M}$  in PBS, pH 6.0) were applied to well for 1 h at 4 °C. After washing with PBST, bound proteins were detected with labeling of mouse anti-c-myc 9e10 mAb (Ig Therapy, Chunchun, Korea) and alkaline phosphatase-conjugated goat anti-mouse mAb (Sigma) and then incubation with *p*-nitrophenylphosphate (Sigma) [18]. Absorbance was read at 405 nm on a VersaMax microplate reader (Molecular devices, Crawley, UK). In pH-dependent binding ELISAs, all experiments were performed with a fixed amount of shFcRn (5  $\mu\text{M}$ ) as described above, except for using PBS with pHs ranging from 5.0 to 8.0.

### 2.8. Surface plasmon resonance (SPR)

Kinetic interactions of shFcRn with hlgGs, mIgG, and TNF $\alpha$  antagonists were performed at 25 °C using a Biacore 2000 SPR biosensor (Pharmacia, Sweden), as previously described [17,18]. After immobilization of shFcRn onto the carboxymethylated dextran surface of a CM5 sensor chip at a level of about 500 response units (RUs), various concentrations (0.32 nM–5  $\mu\text{M}$ ) of each protein (hlgGs, mIgG and TNF $\alpha$  antagonists) prepared by serial dilution with PBST (pH 6.0 or 7.4) were injected into the flow cell at a flow rate of 30  $\mu\text{l}/\text{min}$  for 4 min [4,12]. The running buffer used in the experiments was the same as the protein diluent buffer. Data were zero adjusted after subtraction of the reference cell signal using BIAevaluation software. All kinetic parameters, dissociation ( $k_{\text{off}}$ ) and association ( $k_{\text{on}}$ ) rate constants and equilibrium dissociation constant ( $K_{\text{D}}$ ), were determined by nonlinear regression analysis according to a 1:1 binding model using the BIAevaluation version 3.2 software provided by manufacturer [17,18].

## 3. Results and discussion

### 3.1. Design of a two-promoter vector and transformation into *P. pastoris*

As a eukaryote, the methylotrophic yeast *P. pastoris* offers several advantages in protein expression, including rapid microbial growth and extracellular secretion of correctly folded proteins due to the eukaryotic protein folding and quality control machinery in the endoplasmic reticulum [19]. We designed a two-promoter expression vector pPICZ $\alpha$ A- $\alpha\text{FcRn}$ - $\beta 2\text{m}$ , which co-expresses  $\alpha\text{FcRn}$  and  $\beta 2\text{m}$  by their respective AOX1 promoters in a single vector in *Pichia* (Fig. 1A). Compared with a bicistronic vector system in which the expression of two genes are controlled by a single promoter, the two-promoter vector system can co-express two genes at similar levels in a manner independent of the order of the target genes [20,21]. Thus the two-promoter vector system has been successfully adopted for the heterologous production of binary protein complexes in bacteria [20,21]. However, functional expression of recombinant shFcRn in mammalian cells has been reported using dual-vector systems, where  $\alpha\text{FcRn}$  and  $\beta 2\text{m}$  are co-expressed from two different vectors [4,6,7,9,10]. Using the two-promoter vector system, we intended to optimize the balance of  $\alpha\text{FcRn}$  and  $\beta 2\text{m}$  expression to achieve high levels of the heterodimeric formation by non-covalent interaction to form complete shFcRn along the yeast secretion pathway.

The pPICZ $\alpha$ A- $\alpha\text{FcRn}$ - $\beta 2\text{m}$  plasmid was digested with *Pme* I to generate linearized DNA and transformed into *P. pastoris* by electroporation. After selecting a *Pichia* transformant showing the highest expression level of shFcRn, the transformant was analyzed by genomic PCR to confirm the site specific integration of the plasmid into the genome using a primer set annealing to the upstream of the AOX1 gene on the chromosome [16] and the 3'-terminus region of  $\alpha\text{FcRn}$  in the plasmid (Fig. 1B). A 1.7-kb band was amplified by PCR only in the transformant, but not in untransformed, control yeasts, indicative of the plasmid integration at the genomic AOX1 gene. In addition, the 2.4-kb PCR product from the integrated plasmid sequences (including  $\alpha\text{FcRn}$  and  $\beta 2\text{m}$  coding segment) was amplified only in the transformant, but not in untransformed yeasts. These results demonstrated that the plasmid was correctly integrated into the target site of *Pichia* genome.

### 3.2. Expression and purification of shFcRn in *P. pastoris*

From the chosen transformant, shFcRn was expressed and purified from the culture supernatants using 6 $\times$ His tag, which was

fused only at the C-terminus of  $\beta 2m$ , but not at  $\alpha FcRn$  (Fig. 1A). The purified protein showed two bands with apparent molecular masses of  $\sim 32$  kDa and  $\sim 15$  kDa, corresponding to the  $\alpha FcRn$  and  $\beta 2m$ , respectively, in non-reducing SDS-PAGE analysis (Fig. 2A), demonstrating that the co-expressed  $\alpha FcRn$  and  $\beta 2m$  formed the heterodimeric shFcRn by non-covalent interactions in the culture supernatants.

shFcRn has only one potential N-linked glycosylation site in  $\alpha FcRn$  [9]. There was no significant difference between the theoretical ( $\sim 33$  kDa) and SDS-PAGE-determined ( $\sim 32$  kDa) molecular masses (Fig. 2A). To further evaluate glycosylation status of  $\alpha FcRn$  as a result of *Pichia* expression, the purified proteins were treated with endoglycosidase PNGase F prior to SDS-PAGE analysis. For a control of Infliximab mAb that has a single N-glycosylation site at Asn297 residue of the heavy chain, PNGase F treatment shifted the heterogeneous smear bands into a single band corresponding to the deglycosylated heavy chain band (Fig. 2B). In contrast, the migration pattern and position of  $\alpha FcRn$  were not substantially affected by PNGase F treatment (Fig. 2B), indicative of little or no glycosylation in  $\alpha FcRn$  expressed in *Pichia*. The purification yield of shFcRn was  $\sim 0.8 \pm 0.2$  mg per 1-liter flask culture.

### 3.3. Assembly and secondary structure determination of shFcRn

To investigate the oligomerization state in native conditions, the purified shFcRn was analyzed by SEC. The purified protein was eluted with a single symmetrical major peak at an apparent molecular mass corresponding to the heterodimeric shFcRn ( $\sim 51$  kDa) composed of  $\alpha FcRn$  and  $\beta 2m$  (Fig. 3A). In the presence

of 6 M urea, however, the purified proteins dissociated into two components with apparent molecular masses of  $\sim 35$  kDa ( $\alpha FcRn$ ) and  $\sim 13$  kDa ( $\beta 2m$ ), in good agreement with the non-reducing SDS-PAGE analysis. This result demonstrated that the purified shFcRn exists in a non-covalently associated heterodimeric form in solution.

Secondary structures of the purified shFcRn, determined by far-UV CD spectroscopy, exhibited a negative maximal peak around 217–218 nm and a positive peak at 195–197 nm (Fig. 3B), which is typical for shFcRn with primarily  $\beta$ -sheet and minor  $\alpha$ -helix secondary structures [9,12]. This data suggested that the shFcRn purified from *Pichia* expression was correctly folded.

### 3.4. Functional characterization of shFcRn

The hallmark characteristic of the hlgGs-shFcRn interaction is the strict dependence of its binding on pH [1,2]. To analyze whether the purified shFcRn can bind to hlgGs in a pH-dependent manner, we determined the binding activity of shFcRn with the four subclasses of hlgG in various pHs ranged from 5.0 to 8.0 by ELISA. shFcRn showed the typical pH-dependent binding profiles with hlgGs, exhibiting strong binding to hlgGs between pH 5.0 and 6.0 and decreased binding between pH 6.4 and 6.8, but negligible binding at pHs over 7.2 (Fig. 4A). However, shFcRn did not bind to mIgG at all pHs tested, confirming that there was no cross-reactivity of shFcRn with mIgG [1,11,12]. The  $pH_{50s}$ , pH showing a 50% binding activity, were  $\sim 6.3$ – $6.5$  for the four hlgG subclasses, consistent with shFcRn prepared from CHO cells [4,7]. Thus the shFcRn expressed in *Pichia* maintained the characteristic

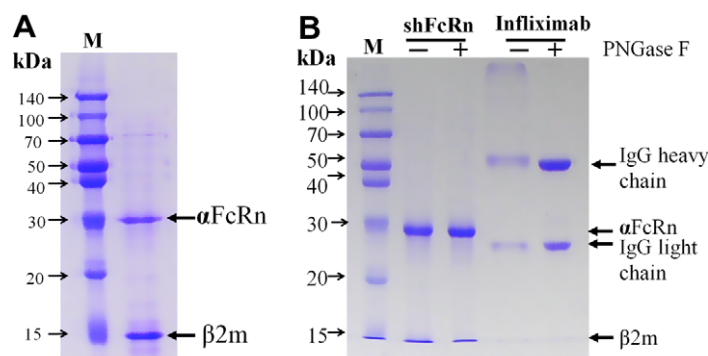


**Fig. 2.** Expression and purification of shFcRn from the culture supernatants of *P. pastoris* transformant. (A) Non-reducing SDS-PAGE analysis of the purified shFcRn ( $\sim 5$   $\mu$ g) from the culture supernatants. (B) Analysis of glycosylation status of shFcRn by PNGase F treatment. Samples, including shFcRn and Infliximab, were treated with (+) or without (-) endoglycosidase PNGase F prior to SDS-PAGE analysis. In (A) and (B), the bands for  $\alpha FcRn$  ( $\sim 32$  kDa) and  $\beta 2m$  ( $\sim 15$  kDa) of shFcRn as well as for the IgG heavy chain ( $\sim 50$  kDa) and IgG light chain ( $\sim 25$  kDa) of Infliximab were indicated by arrows. Samples were separated on a 12% SDS polyacrylamide gel under the non-reducing (A) and reducing (B) conditions and visualized by staining with Coomassie Blue R-250. The molecular mass markers are indicated in kDa.

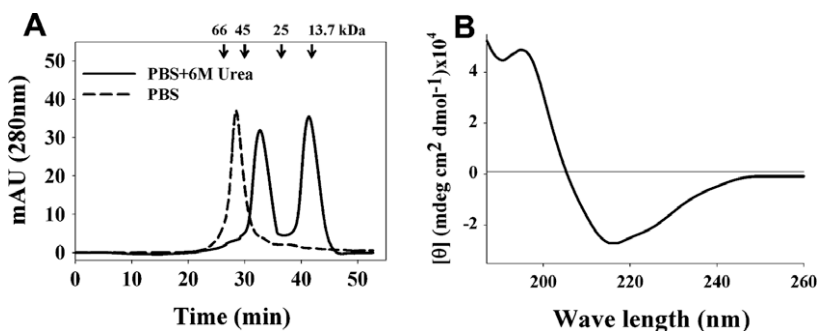


**Fig. 3.** Biochemical characterization of the purified shFcRn from *Pichia*. (A) Size exclusion elution profile of shFcRn (100  $\mu$ g/ml) in native (dotted line) and dissociated (solid line) states, monitored at 280 nm. shFcRn incubated in PBS (pH 7.4) with or without 6 M urea for 2 h at 25  $^{\circ}$ C was injected in a volume of 100  $\mu$ l. The arrows indicate the elution positions of molecular weight standards (alcohol dehydrogenase, 150 kDa; bovine serum albumin, 66 kDa; ovalbumin, 45 kDa; chymotrypsinogen, 25 kDa; ribonuclease, 13.7 kDa), including blue dextran 2000 ( $\sim 2000$  kDa) as a void volume marker. (B) Far-UV CD spectrum of shFcRn (100  $\mu$ g/ml in PBS, pH 7.4) to monitor the secondary structure.

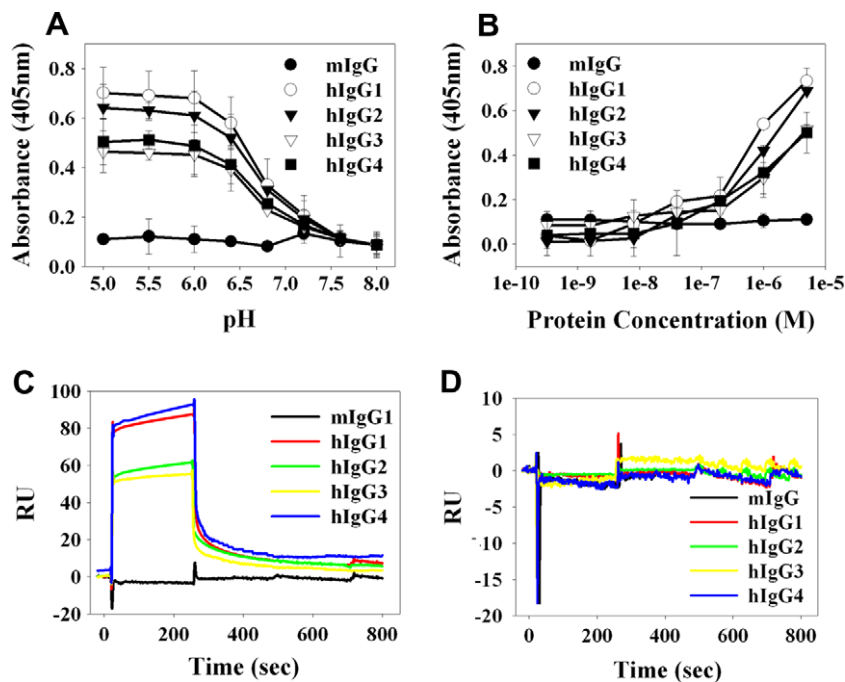


**Fig. 4.** Functional characterization of the purified shFcRn from *Pichia*. (A) pH-dependent binding profiles of shFcRn with the four subclasses of hIgG between pH 5.0 and 8.0, determined by ELISA. (B) Concentration-dependent binding activities of shFcRn with the four hIgG subclasses at acidic pH 6.0, determined by ELISA. In (A) and (B), ELISA plates were coated with 1  $\mu\text{g}/\text{ml}$  of each hIgG and then incubated with 5  $\mu\text{M}$  shFcRn in PBS with the indicated various pHs (A) or the serially diluted concentrations of shFcRn in PBS with pH 6.0 (B). Bound shFcRn was detected by mouse anti-myc mAb. (C and D) Representative SPR sensorgrams for the interactions of the four hIgG subclasses with shFcRn at pH 6.0 (C) and 7.4 (D). Each hIgG (5  $\mu\text{M}$ ) was injected over shFcRn-immobilized surface at a density of 500 RU in running and elution buffer conditions of pH 6.0 or 7.4. In (A–D), mIgG was employed as a negative control.

pH-dependent interactions with hIgGs without cross-reactivity with mIgG, which is critical for their function in regulating the levels of hIgGs in circulation [1,2], strongly suggesting that it was functionally expressed and purified from the *Pichia* expression system.

IgG in humans contains four subclasses, designated as IgG1, IgG2, IgG3, and IgG4, which have  $\sim 90\%$  homology in their amino acid sequences in the Fc regions [1,2]. To measure their relative binding affinities with shFcRn, the concentration-dependent binding activity of shFcRn for the four hIgG subclasses was determined by ELISA at an acidic pH 6.0. As shown in Fig. 4B, shFcRn showed a binding preference in the order  $\text{hIgG1} \geq \text{hIgG2} > \text{hIgG3} \geq \text{hIgG4}$ , similar to the profiles for shFcRn expressed in CHO cells [9]. The binding interactions of shFcRn with hIgGs were further quantified by SPR technique, which was performed at pH 6.0 and 7.4. Consistent with ELISA, SPR experiments showed that hIgGs, but not mIgG, bound to shFcRn only at pH 6.0 with no substantial binding at pH 7.4 (Fig. 4C and D). The interactions of hIgGs with shFcRn exhibited very fast association and dissociation phases (Fig. 4C), which was typical of their interactions [4,7,11,12].

### 3.5. Binding characterizations of shFcRn with TNF $\alpha$ antagonists

TNF $\alpha$ -blocking therapy using biologic TNF $\alpha$  antagonists, including Infliximab, Adalimumab, and Etanercept, has been approved for the treatment of several diseases including rheumatoid arthritis, psoriasis and Crohn's disease [15]. While Infliximab and Adalimumab are full-length, bivalent hIgG1 mAbs, Etanercept is a genetically engineered fusion protein composed of a dimer of the extracellular portions of human TNF receptor 2 (TNFR2) fused to the Fc portion of hIgG1 [14,15]. Although the amino acid sequences of the Fc regions are known to be identical with those of Infliximab and Adalimumab, Etanercept shows a markedly shorter serum half-life ( $\sim 4$  days) than the mAbs of Infliximab (8–10 days) and

Adalimumab (10–20 days) in humans [15]. hFcRn salvages a large fraction ( $\sim 60\%$ ) of hIgGs endocytosed by fluid-phase pinocytosis from lysosomal degradation in endothelial cells [22], resulting in increased hIgG serum persistence *in vivo* [1,2]. Increased affinity of Fc-containing TNF $\alpha$  antagonists for the FcRn at pH 6.0 would shift the equilibrium toward the recycling pathway, thereby translating to improved *in vivo* pharmacokinetics [8,22]. However, there have been no studies comparing the binding affinities of the TNF $\alpha$  antagonists with shFcRn.

To determine whether the shFcRn binding affinity of the TNF $\alpha$  antagonists, Infliximab, Adalimumab, and Etanercept, correlates with their different serum half-lives, we first evaluated the pH-dependent binding interactions with shFcRn by ELISA. All of the TNF $\alpha$  antagonists displayed improved shFcRn binding activities at acidic pH at lower than pH 6.5 with no significant binding at pH more than 7.2, exhibiting  $\text{pH}_{50\%} \sim 6.4\text{--}6.8$  (Fig. 5A). The analyses of their concentration-dependent binding activity revealed that shFcRn bound more strongly to Infliximab and Adalimumab mAbs than to Etanercept (Fig. 5B). To obtain more quantitative binding affinities, SPR experiments were performed by injecting various concentrations of each TNF $\alpha$  antagonist over shFcRn-immobilized surface at pH 6.0. The apparent  $K_{\text{D}}$ s of shFcRn for Infliximab, Adalimumab, and Etanercept were  $\sim 396$  nM,  $\sim 411$  nM, and  $\sim 1.92$   $\mu\text{M}$ , respectively (Table 2), demonstrating that shFcRn at pH 6.0 bound to Infliximab and Adalimumab mAbs with 10-fold higher binding affinity than to Etanercept. The  $K_{\text{D}}$  values of the shFcRn from *Pichia* are comparable to those (2.52  $\mu\text{M} \sim 12$  nM) obtained for hIgG1 binding to shFcRn prepared from insect and CHO cells [9,11,12]. The plotting of the maximal RU ( $\text{RU}_{\text{max}}$ ) of the sensorgram obtained by various concentrations of each TNF $\alpha$  antagonist confirmed that shFcRn bound to Infliximab and Adalimumab mAbs with higher affinity than Etanercept (Fig. 5C). At pH 7.4, no binding of the three TNF $\alpha$  antagonists to shFcRn was observed even by the highest concentration injection (5  $\mu\text{M}$ ) used for pH 6.0 binding.

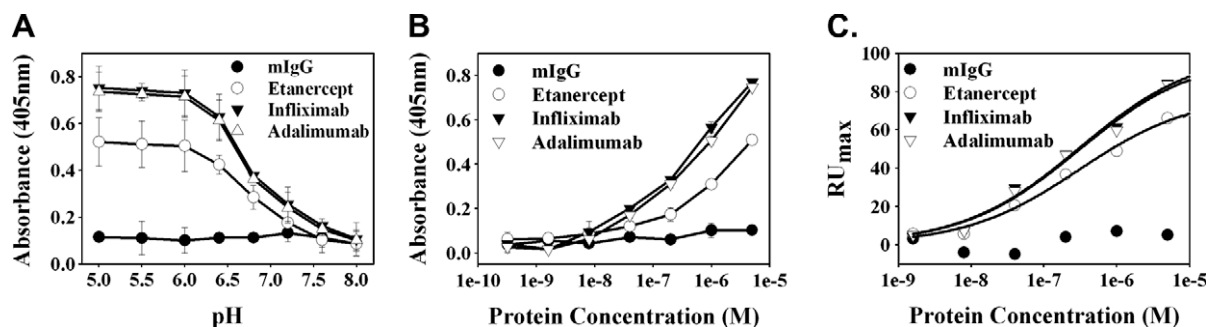


**Fig. 5.** Binding analyses of the shFcRn with the three TNF $\alpha$  antagonists, Infliximab, Adalimumab, and Etanercept. (A) pH-dependent binding profiles of shFcRn with the TNF $\alpha$  antagonists between pH 5.0 and 8.0, determined by ELISA. (B) Concentration-dependent binding profiles of shFcRn with each TNF $\alpha$  antagonist at acidic pH 6.0, determined by ELISA. In (A) and (B), ELISA plates were coated with 1  $\mu$ g/ml of each TNF $\alpha$  antagonist and then incubated with 5  $\mu$ M shFcRn in PBS with the indicated various pHs (A) or the serially diluted concentrations of shFcRn in PBS with pH 6.0 (B). Bound shFcRn was detected by mouse anti-myc mAb. (C) Concentration-dependent binding profiles of each TNF $\alpha$  antagonist with shFcRn at pH 6.0, determined by SPR. Maximal RU (RU<sub>max</sub>) values of SPR sensorgrams obtained by injection of various concentrations of each TNF $\alpha$  antagonist over shFcRn-immobilized surface at a density of 500 RU in running and elution buffer condition of pH 6.0 were plotted against the injected concentrations of each TNF $\alpha$  antagonist. In (A–C), mIgG was employed as a negative control.

**Table 2**

The kinetic interaction parameters for the interactions of shFcRn and the three TNF $\alpha$  antagonists, Infliximab, Adalimumab, and Etanercept, determined by SPR.<sup>a</sup>

Analyte protein	$k_{on}$ ( $M^{-1}s^{-1}$ )	$k_{off}$ ( $s^{-1}$ )	$K_D$ (M)
Infliximab	$7.63 \pm 0.53 \times 10^3$	$3.03 \pm 0.22 \times 10^{-3}$	$3.96 \pm 0.32 \times 10^{-7}$
Adalimumab	$8.06 \pm 0.51 \times 10^3$	$3.31 \pm 0.19 \times 10^{-3}$	$4.11 \pm 0.25 \times 10^{-7}$
Etanercept	$2.24 \pm 0.09 \times 10^3$	$4.31 \pm 0.15 \times 10^{-3}$	$1.92 \pm 0.08 \times 10^{-6}$

<sup>a</sup> At least five data sets were used in the determination of the constants and the values are represented as mean  $\pm$  SD from at least two different experiments.

At this point, it is not clear why Etanercept exhibited a lower affinity with shFcRn than Infliximab and Adalimumab mAbs did, even though they have the same amino acid sequence in the Fc region of hIgG1 [15]. One possibility is the glycosylation at the C-terminus of TNFR2 immediately before the Fc region of Etanercept. The glycosylation might induce the Fc conformation to be slightly different from that of Infliximab and Adalimumab or steric hindrance for shFcRn accessibility to the Fc region, resulting in the lower binding activity of Etanercept for shFcRn than the mAbs. Even though the direct co-relationship between increased binding affinity of hIgGs to hFcRn and improved pharmacokinetic properties are controversial [4,6–8], our results suggest that the shorter serum half-life of Etanercept might be explained by the lower affinity with hFcRn, compared with the counter IgG1 mAbs.

#### 4. Conclusion

Here, we demonstrated a soluble and functional expression of shFcRn in *P. pastoris* using the two-promoter vector system, where  $\alpha$ FcRn and  $\beta$ 2m are co-expressed under their respective promoters in a single vector. This strategy may be useful for the production of other eukaryotic binary protein complexes. The  $\alpha$ FcRn and  $\beta$ 2m purified together from the culture supernatants was correctly assembled to form the heterodimeric shFcRn with the typical secondary structures. The shFcRn showed the characteristic typical pH-dependent binding activity for the four subclasses of hIgG without cross-reactivity with mIgG, which is comparable to those of shFcRn prepared by mammalian cell expression. The shFcRn was further exploited to determine the different binding affinities with the TNF $\alpha$  antagonists, providing a clue to their different serum half-lives in human. Our results provide a functional expression system of shFcRn in *Pichia*, which can be used for biochemical and biological studies of hFcRn and as a screening probe for the Fc engineering of hIgGs.

#### Acknowledgments

This work was supported by grants from the KRIBB, the basic research (KRF-2007-313-D00248), the Converging Research Center Program (2009-0093653), and Priority Research Centers Program (2009-0093826) from the National Research Foundation of the Ministry of Education, Science and Technology, and the BioGreen 21 Program (20070401034007) from the Rural Development Administration, Republic of Korea.

#### References

- D.C. Roopenian, S. Akilesh, FcRn: the neonatal Fc receptor comes of age, *Nat. Rev. Immunol.* 7 (2007) 715–725.
- V. Ghetie, E.S. Ward, Multiple roles for the major histocompatibility complex class I-related receptor FcRn, *Annu. Rev. Immunol.* 18 (2000) 739–766.
- R. Szlauer, I. Ellinger, S. Haider, L. Saleh, B.L. Busch, M. Knofler, R. Fuchs, Functional expression of the human neonatal Fc-receptor, hFcRn, in isolated cultured human syncytiotrophoblasts, *Placenta* 30 (2009) 507–515.
- A. Datta-Mannan, D.R. Witcher, Y. Tang, J. Watkins, W. Jiang, V.J. Wroblewski, Humanized IgG1 variants with differential binding properties to the neonatal Fc receptor: relationship to pharmacokinetics in mice and primates, *Drug Metab. Dispos.* 35 (2007) 86–94.
- M. Raghavan, V.R. Bonagura, S.L. Morrison, P.J. Bjorkman, Analysis of the pH dependence of the neonatal Fc receptor/immunoglobulin G interaction using antibody and receptor variants, *Biochemistry* 34 (1995) 14649–14657.
- W.F. Dall'Acqua, P.A. Kiener, H. Wu, Properties of human IgG1s engineered for enhanced binding to the neonatal Fc receptor (FcRn), *J. Biol. Chem.* 281 (2006) 23514–23524.
- A. Datta-Mannan, D.R. Witcher, Y. Tang, J. Watkins, V.J. Wroblewski, Monoclonal antibody clearance. Impact of modulating the interaction of IgG with the neonatal Fc receptor, *J. Biol. Chem.* 282 (2007) 1709–1717.
- P.R. Hinton, J.M. Xiong, M.G. Johlf, M.T. Tang, S. Keller, N. Tsurushita, An engineered human IgG1 antibody with longer serum half-life, *J. Immunol.* 176 (2006) 346–356.
- A.P. West Jr., P.J. Bjorkman, Crystal structure and immunoglobulin G binding properties of the human major histocompatibility complex-related Fc receptor, *Biochemistry* 39 (2000) 9698–9708.
- S. Popov, J.G. Hubbard, J. Kim, B. Ober, V. Ghetie, E.S. Ward, The stoichiometry and affinity of the interaction of murine Fc fragments with the MHC class I-related receptor, FcRn, *Mol. Immunol.* 33 (1996) 521–530.
- M. Firan, R. Bawdon, C. Radu, R.J. Ober, D. Eaken, F. Antohe, V. Ghetie, E.S. Ward, The MHC class I-related receptor, FcRn, plays an essential role in the maternofetal transfer of gamma-globulin in humans, *Int. Immunol.* 13 (2001) 993–1002.
- J.T. Andersen, S. Justesen, G. Berntzen, T.E. Michaelsen, V. Lauvrak, B. Fleckenstein, S. Buus, I. Sandlie, A strategy for bacterial production of a soluble functional human neonatal Fc receptor, *J. Immunol. Methods* 331 (2008) 39–49.
- A. Gallimore, A. Glithero, A. Godkin, A.C. Tissot, A. Pluckthun, T. Elliott, H. Hengartner, R. Zinkernagel, Induction and exhaustion of lymphocytic choriomeningitis virus-specific cytotoxic T lymphocytes visualized using soluble tetrameric major histocompatibility complex class I-peptide complexes, *J. Exp. Med.* 187 (1998) 1383–1393.
- M.S. Kim, S.H. Lee, M.Y. Song, T.H. Yoo, B.K. Lee, Y.S. Kim, Comparative analyses of complex formation and binding sites between human tumor necrosis factor- $\alpha$  and its three antagonists elucidate their different neutralizing mechanisms, *J. Mol. Biol.* 374 (2007) 1374–1388.

- [15] D. Tracey, L. Klareskog, E.H. Sasso, J.G. Salfeld, P.P. Tak, Tumor necrosis factor antagonist mechanisms of action: a comprehensive review, *Pharmacol. Ther.* 117 (2008) 244–279.
- [16] K. De Schutter, Y.C. Lin, P. Tiels, A. Van Hecke, S. Glinka, J. Weber-Lehmann, P. Rouze, Y. Van de Peer, N. Callewaert, Genome sequence of the recombinant protein production host *Pichia pastoris*, *Nat. Biotechnol.* 27 (2009) 561–566.
- [17] D.S. Kim, S.H. Lee, J.S. Kim, S.C. Lee, M.H. Kwon, Y.S. Kim, Generation of humanized anti-DNA hydrolyzing catalytic antibodies by complementarity determining region grafting, *Biochem. Biophys. Res. Commun.* 379 (2009) 314–318.
- [18] E.S. Sung, K.J. Park, S.H. Lee, Y.S. Jang, S.K. Park, Y.H. Park, W.J. Kwag, M.H. Kwon, Y.S. Kim, A novel agonistic antibody to human death receptor 4 induces apoptotic cell death in various tumor cells without cytotoxicity in hepatocytes, *Mol. Cancer Ther.* 8 (2009) 2276–2285.
- [19] K. Graumann, A. Premstaller, Manufacturing of recombinant therapeutic proteins in microbial systems, *Biotechnol. J.* 1 (2006) 164–186.
- [20] D.P. Humphreys, B. Carrington, L.C. Bowering, R. Ganesh, M. Sehdev, B.J. Smith, L.M. King, D.G. Reeks, A. Lawson, A.G. Popplewell, A plasmid system for optimization of Fab' production in *Escherichia coli*: importance of balance of heavy chain and light chain synthesis, *Protein Expr. Purif.* 26 (2002) 309–320.
- [21] K.J. Kim, H.E. Kim, K.H. Lee, W. Han, M.J. Yi, J. Jeong, B.H. Oh, Two-promoter vector is highly efficient for overproduction of protein complexes, *Protein Sci.* 13 (2004) 1698–1703.
- [22] J. Kim, W.L. Hayton, J.M. Robinson, C.L. Anderson, Kinetics of FcRn-mediated recycling of IgG and albumin in human: pathophysiology and therapeutic implications using a simplified mechanism-based model, *Clin. Immunol.* 122 (2007) 146–155.